

# 1 Carbon balance and emissions of methane and nitrous oxide during 2 four years of moderate rewetting of a cultivated peat soil site 3

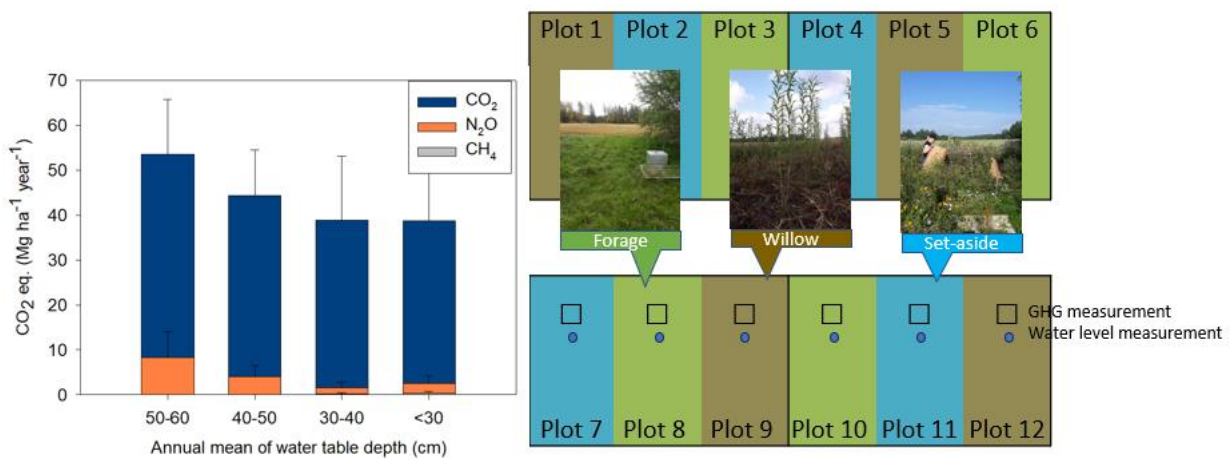
4 Kristiina Lång\*, Henri Honkanen, Jaakko Heikkinen, Sanna Saarnio, Tuula Larmola, Hanna Kekkonen  
5 Natural Resources Institute Finland, Latokartanonkaari 9, FI-00790 Helsinki, Finland

6 *Correspondence to:* Kristiina Lång (kristiina.lang@luke.fi)  
7

8 **Abstract.** Raising the water table is an effective way to abate greenhouse gas emissions from cultivated peat soils. We  
9 experimented a gradual water table rise at a highly degraded agricultural peat soil site with plots of willow, forage and mixed  
10 vegetation (set-aside) in southern Finland. We measured the emissions of carbon dioxide (CO<sub>2</sub>), methane (CH<sub>4</sub>) and nitrous  
11 oxide (N<sub>2</sub>O) for four years. The mean annual ground water table depth was about 80, 40, 40 and 30 cm in 2019-2022,  
12 respectively. The results indicated that a 10 cm raise in the water table depth was able to slow down annual CO<sub>2</sub> emissions  
13 from soil respiration by 0.87 Mg CO<sub>2</sub>-C ha<sup>-1</sup>. CH<sub>4</sub> fluxes changed from uptake to emissions with a raise in the water table  
14 depth, and the maximum mean annual emission rate was 11 kg CH<sub>4</sub>-C ha<sup>-1</sup>. Nitrous oxide emissions ranged from 2 to 33 kg  
15 N<sub>2</sub>O-N ha<sup>-1</sup> year; they were high from bare soil in the beginning of the experiment but decreased towards the end of the  
16 experiment. Short rotation cropping of willow reached net sequestration of carbon before harvest, but all treatments and years  
17 showed net loss of carbon based on the net ecosystem carbon balance. Overall, the short rotation coppice of willow had the  
18 most favourable carbon and greenhouse gas balance over the years (10 Mg CO<sub>2</sub> equivalent on the average over four years).  
19 The total greenhouse gas balance of the forage and set-aside treatments did not go under 27 Mg CO<sub>2</sub> equivalent ha<sup>-1</sup> year<sup>-1</sup>  
20 highlighting the challenge in curbing peat decomposition in highly degraded cultivated peatlands.  
21

22 Keywords: peatland, greenhouse gas, ground water table, paludiculture, land use  
23

24 Graphical abstract



Photos: Jaana Nissi

25  
26  
27  
28

## 29 **1. Introduction**

30 Cultivated peatlands are a major source of greenhouse gas (GHG) emissions globally (Strack et al., 2022). Conventional  
31 cultivation requires lowering the water table depth (WTD) which makes all peat above the drainage depth prone to microbial  
32 decomposition. Intensive management together with the high carbon and nitrogen content of peat makes agricultural peat  
33 soils the highest CO<sub>2</sub> and N<sub>2</sub>O emitters per unit area compared to any other land use types on peat soils (Maljanen et al.,  
34 2010). Their GHG emissions currently diminish the net carbon sink of peat-rich countries significantly which can also be  
35 turned to an advance: the climate change mitigation potential of drained peatlands is high (Humpenöder et al., 2020; Leifeld  
36 and Menichetti, 2018) and cost per mitigated unit of CO<sub>2</sub> equivalent low (Lehtonen et al., 2022).

37 WTD is the major controller of GHG fluxes from peat soils (Evans et al., 2021; Wilson et al., 2016). A global meta-analysis  
38 on water table manipulation studies showed that WTD explained most of the variation in GHG emissions but e.g. climate  
39 zone had some influence as well (Huang et al., 2021). Rewetting has been found to diminish the release of CO<sub>2</sub> and N<sub>2</sub>O from  
40 decomposition but the switch from aerobic to anaerobic decomposition may change the ecosystem from a sink to source of  
41 CH<sub>4</sub>. However, the average increase in CH<sub>4</sub> emissions usually does not compromise the net GHG mitigation potential (Bianchi  
42 et al., 2021; Guenther et al., 2020; Mander et al., 2023) but data is needed to understand the factors regulating CH<sub>4</sub> emissions  
43 that can sometimes be high after rewetting (Nielsen et al., 2023).

44 Paludiculture, i.e. crop production in wet conditions on peat soils, is a GHG mitigation method that allows for slowing down  
45 peat decomposition while still maintaining agricultural income from peatlands for the landowner (Tanneberger et al., 2022).  
46 It is an opportunity for the agribusiness to improve the overall sustainability (Freeman et al., 2022; Liu et al., 2023) and it  
47 produces clearly more societal benefits regarding ecosystem services than conventional management (Liu et al., 2023). As  
48 regards to GHG mitigation, the raise in WTD reduces carbon losses from peat decomposition but export of carbon in the  
49 harvest impairs the carbon balance of the system (Beetz et al., 2013). Emissions of N<sub>2</sub>O are generally found to be low in  
50 paludiculture (Bianchi et al., 2021) but they can remain high if fertilisers are applied (Bockermann et al., 2024). Emissions  
51 of CH<sub>4</sub> are affected by the crop type, harvest management and N fertilisation (Boonman et al., 2023) but they can be efficiently  
52 reduced by leaving an oxidised, non-waterlogged, layer on the peat surface to facilitate microbial oxidation of CH<sub>4</sub> (Kandel  
53 et al., 2020). Solutions for paludiculture implementation are e.g. forage and willow that can be produced in wet conditions  
54 because their roots improve the bearing capacity of the peat and thus ease machine work in wet conditions. Compared to  
55 restoration to natural conditions, paludiculture leads to compromises, as both ecosystem services and economic productivity  
56 are expected to be maintained, and it is not well known how these two aspects are best harmonised in practice. Set-aside is  
57 often not a planned management option, but wet fields drift to non-productive use when the drainage system degrades, and  
58 there are limited data on the GHG balance of such fields.

59 We established an experimental site with forage, willow and set-aside treatments in wet management on highly decomposed  
60 cultivated peat soil in southern Finland in 2019-2023. As the target WTD of -20 cm below the surface was reached only  
61 periodically, we cannot call the site a paludiculture site, but the results can be used to discuss the effects and practical issues  
62 during the transition period to paludiculture. Our research questions were 1) What is the carbon and GHG balance of a  
63 moderately rewetted drained peatland, 2) How much does harvesting reduce the potential to improve the carbon balance and  
64 3) Do CH<sub>4</sub> emissions compromise the GHG mitigation in wet management?

## 67 **2. Materials and methods**

### 68 **2.1. The site and management**

69 The site was located in southern Finland (60.22 °N, 24.78 °E, 110 m a.s.l.) and it has been in cultivation at least since the 19<sup>th</sup>  
70 century. The field has been in a crop rotation with cereals and grass during the latest decades. The climate is boreal humid

71 with long term (1991–2021) annual mean temperature of 5.2 °C and precipitation of 621 mm (Jokinen et al. 2021). The sum  
 72 of annual global radiation is 3358 MJ m<sup>-2</sup> and total sunshine duration 1699 hours. Typically, the soil is frozen and has a snow  
 73 cover from December to March-April. The field was a highly decomposed fen with peat depth ranging from 0.8 to over 2 m.  
 74 Organic carbon content was 25% and pH 5.5 in the surface layer (0–20 cm) (Table 1). The original subsurface drainage  
 75 system with tile drains was replaced by modern plastic pipes surrounded by gravel in the 1960s. The distance between the  
 76 pipes was 18 m until 1979 when it was changed to 9 m. The drainage depth was 60–80 cm, and a control well was installed  
 77 prior to the experiment to restrict water outflow and raise the ground water table. The adjustable tube inside the well was set  
 78 to a position letting the water out when the water table reached 20 cm depth below the soil surface.

80 **Table 1:** Soil properties ( $\pm$ standard deviation) in the 0-20 cm layer in 2021

Variable	Value
Decomposition status (von Post)	8 (7-9)
Bulk density (g cm <sup>-3</sup> )	0.39 $\pm$ 0.05
Porosity (%)	0.80 $\pm$ 0.02
Ash (%)	42 $\pm$ 3.8
pH	5.4 $\pm$ 0.09
C (g kg <sup>-1</sup> )	286 $\pm$ 24.6
N (g kg <sup>-1</sup> )	15.2 $\pm$ 1.24
Tot P (g kg <sup>-1</sup> )	0.97 $\pm$ 0.08
Soluble P (g kg <sup>-1</sup> )	0.01 $\pm$ 0.001
K (g kg <sup>-1</sup> )	0.17 $\pm$ 0.03
Mn (g kg <sup>-1</sup> )	0.15 $\pm$ 0.02
S (g kg <sup>-1</sup> )	2.01 $\pm$ 0.13
Al (g kg <sup>-1</sup> )	1.41 $\pm$ 0.12
Fe (g kg <sup>-1</sup> )	5.92 $\pm$ 0.63

81  
 82 The site was established in 2018 and it consists of twelve experimental plots (9 × 6 m) in four blocks (see the graphical  
 83 abstract). Four replicate plots with either grass mixture for forage (sown with *Poa trivialis* and *Festuca pratensis*, replanted  
 84 in 2019 and 2021 with *Phleum pratense*, *Festuca pratensis*, *Lolium multiflorum* and *Poa pratensis*), bog bilberry (*Vaccinium*  
 85 *uliginosum*; aka bog blueberry or bog whortleberry) or willow variety Klara (hybrid of *Salix schwerinii* Amgunkaja x *Salix*  
 86 *viminialis* Ivar) were randomly assigned within the four blocks. The grass was seeded and bilberry seedlings and willow  
 87 saplings planted in June 2018 (Table S1). The bilberry did not grow roots, and those plots were left to develop to set-aside  
 88 during the following years, thus we named this treatment as “set-aside”. The number of species in all twelve plots was  
 89 determined once in the summer 2021.

## 91 2.2 Ancillary measurements

92 Biomass growth of willow was monitored by cutting three willow individuals from each plot for determining the above-  
 93 ground biomass each June. The leaves, and stem + branches were separated and weighed to determine the fresh biomass. The  
 94 woody biomass was cut in 10 cm pieces and dried at 65 °C for two weeks. The root biomass around one of the monitored  
 95 plants per plot was determined by taking 50 × 80 × 20 cm peat samples from three layers: 0–20, 20–40 and 40–60 cm once  
 96 per year. Visible large (>2 mm) and fine roots were manually separated from the peat, dried and weighed. For determining  
 97 fine roots, the peat samples were mixed, and a 1 kg subsample was taken. Annual growth in stem, stool and coarse roots was  
 98 calculated by subtracting the value from the previous year. Annual turnover rate of fine roots was assumed to be three times  
 99 the biomass of fine roots as in Pacaldo et al. (2014). For example, biomass increment in 2019 was calculated with the  
 100 following equation:

$$102 \text{ Annual Growth} = F_{19} + (S_{20} - S_{19}) + (St_{20} - St_{19}) + (Cr_{20} - Cr_{19}) + 3 * Fr_{19} \quad (1)$$

104 , where F19 is foliage in 2019, S19 and S20 are stems in 2019 and 2020, St19 and St20 are stools in 2019 and 2020, Cr19  
105 and Cr20 are coarse roots in 2019 and 2020 and Fr19 is fine roots in 2019. Subsamples were taken for determining the C  
106 content of the dried biomass in 2019 and 2020, and the mean values were used for the following years. The yield per hectare  
107 was estimated to be the weight of 25,000 individuals, based on 80 cm × 50 cm spacing.

108 Soil temperature was measured first at the depth of 10 cm (but at the depth of 5 cm from May 2020 on to achieve better  
109 response of CO<sub>2</sub> to air temperature) in each treatment with Elcolog sensors (Elcoplast Oy, Tampere, Finland). The sampling  
110 rate was one hour in summer and 2.5 hours in winter. The air temperature, precipitation and radiation data were taken from  
111 the [Jokioinen](#) weather station of Finnish Meteorological Institute (FMI [2024](#), CC BY 4.0) located about 10 km from the site.  
112 Continuous photosynthetically active radiation (PAR) data was produced with global radiation data from FMI and corrected  
113 using the ratio of 2.04 for global radiation and the PAR (Meek et al., 1984).

114 WTD was measured from monitoring pipes at the corners of the site at the time of the opaque chamber measurements until  
115 2021 when monitoring pipes were installed also in the centre of each plot. During summers 2021 and 2022, there were also  
116 HOBO Water Level data loggers (Onset, Bourne, United States) in each plot for continuous water level monitoring with a  
117 sampling rate of one hour. In winter when the loggers were not used, WTD was measured manually from monitoring pipes  
118 when the water was not frozen.

119 Leaf area index (LAI) was measured at the same time with the transparent chamber measurements with a portable LAI meter  
120 (SunScan; Delta-T Devices Ltd, Cambridge, United Kingdom). LAI values > 3 were set to 3 as they were assumed to not  
121 affect photosynthesis due to saturation of the reflectance (Aparicio et al., 2000). When harvesting the grass plots, the previous  
122 measured LAI value was extrapolated to the moment just before harvesting, after which the LAI value was set to 1 as  
123 measured. In 2022, we measured green canopy cover [with the Canopeo app \(Patrignani and Ochsner, 2015\)](#) instead of LAI,  
124 ~~because it~~ [Based on our experiences, and due to the operation and physical design of the LAI device, it did not provide as](#)  
125 [comprehensive picture of the biomass inside the gas measurement collar as Canopeo. Vegetation index has been found to be](#)  
126 [faster to measure and less dependent on the ambient light conditions than the light interception method-likely responds better](#)  
127 [to photosynthesis \(Shepherd et al. 2018\). Green canopy cover was measured with the Canopeo app \(Patrignani and Ochsner,](#)  
128 [2015\). LAI was indexed by dividing by maximum value 3 and green canopy cover by 100 \(values from 0% to 100%\) so that  
129 the generated vegetation index range was 0–1. The vegetation index was set to 0 from the end of November until mid-April  
130 when the snow and frost covered the ground or no green vegetation was present.](#)

131 Soil samples for analysing the soil properties were taken first in October 2018 and another sampling was conducted in June  
132 2021 with additional analysis. As there were no significant changes in the soil properties between these samplings, we present  
133 only the results of the second soil sampling in Table 1. The samples were taken from the 0-20 cm layer using a soil corer with  
134 a diameter of 3 cm. Approx. 20 subsamples were pooled to make composite sample that was air-dried and sieved (2 mm) for  
135 the chemical analyses. Soil core samples for dry bulk density and porosity (diameter 5 cm) were taken from the surface layer  
136 (0–17.5 cm) of each plot in Oct 2020 using the Kopec corer, and the samples were dried at 37 °C for a week. Soil acidity was  
137 determined using the ISO 10390 method. Nutrient content was analysed as described in Vuorinen and Mäkitie (1955). Soil  
138 carbon and nitrogen were determined using the dry combustion method (Leco TruMac CN, LECO corporation, MI).

139

### 140 **2.3. GHG measurements**

141 Dark respiration of the plants together with soil respiration (ecosystem respiration) and fluxes of N<sub>2</sub>O and CH<sub>4</sub> were measured  
142 using opaque chambers biweekly or once per month in the winter between 3/2019 – 3/2023. In each plot, a 60 cm × 60 cm  
143 steel collar was installed at the depth of 10–15 cm. The location of the collars was one metre from the short edge of the plot  
144 and three metres from the edges of the adjacent plots. An aluminium chamber (height 40 cm) mounted at the top of the collar  
145 was sealed with water in the groove of the upper edge of the collar. In the winter, NaCl was added to the water to avoid ice  
146 formation. The clear aluminium surface reflected effectively light and kept the temperature change moderate inside the

147 chamber. The measurements were done during the daytime between 10 am and 2 pm approximately every two weeks in  
148 summertime, and monthly in the winter. The chambers were closed for 30 minutes, and four 20 ml gas samples were taken  
149 with a 60-ml plastic syringe to pre-evacuated vials (Exetainer, Labco Limited, UK) in 10-minute intervals starting  
150 immediately after closing. Prior to sampling, the syringe was pumped five times to mix the air in the chamber. The samples  
151 were analysed with a gas chromatograph (Agilent 7890 Agilent Technologies, Inc., Wilmington, DE, USA) equipped with  
152 flame ionizer and electron capture detectors, and a nickel catalyst for converting CO<sub>2</sub> to CH<sub>4</sub>. The gas chromatograph had a  
153 2 ml sample loop and a backflush system for separating water from the sample and flushing the precolumn between the runs.  
154 The precolumn and analytical columns consisted of 1.8 and 3 m long steel columns, respectively, and were packed with  
155 80/100 mesh Hayesep Q (Supelco Inc., Bellefonte, PA, USA). Nitrogen was used as the carrier gas and a standard gas mixture  
156 of known concentration of CO<sub>2</sub>, N<sub>2</sub>O and CH<sub>4</sub> was used for a calibration curve with seven concentration points. An  
157 autosampler (222 XL Liquid handler, Gilson Medical Electronics, France) fed the samples to the loop of the gas  
158 chromatograph.

159 Net ecosystem exchange (NEE) including photosynthesis and respiration of the soil and plants was measured approximately  
160 every two weeks during the growing season using a transparent chamber (60 × 60 × 60 cm) made of polycarbonate plexiglass  
161 (1 mm, light transmission 95%). The chamber was equipped with a Vaisala GMP-343 probe for CO<sub>2</sub> measurement and a  
162 temperature and humidity sensor (Vaisala Oy, Vantaa, Finland) and two fans for mixing the air during the measurement. PAR  
163 was measured with LI-190 quantum PAR sensor (LI-COR, Lincoln, Nebraska, USA) inside the chamber. Four measurements  
164 with different amount of entering light were taken from each plot on each measurement day in order to cover a large range of  
165 light conditions and facilitate the gap filling by modelling. One or two layers of a white fabric shroud and one blackout curtain  
166 were used to acquire measurement results in different light conditions (approximately 100%, 50%, 25%, 0% of ambient  
167 radiation). The measurement with 0% radiation gave the estimate for ecosystem respiration (ER). The measurements were  
168 done in the same collars as the opaque chamber measurements. Each measurement took one minute with a five second  
169 sampling rate, or two minutes in early or late growing season when the change in flux was minor. The chamber was flushed  
170 after each measurement to reconstitute ambient CO<sub>2</sub> and air humidity contents. After closing the chamber, a lag time of 10  
171 seconds was applied to exclude the time when the flux was not yet stabilised. Clear sky conditions were preferred to avoid  
172 problems related to changing cloud cover and to achieve the widest possible range of available light. The temperature change  
173 inside the chamber was less than 1.5 degrees which was also used as a criterion for data filtering.

174 The change of CO<sub>2</sub> concentration during the chamber enclosure was assumed to be linear. The measurement results of CO<sub>2</sub>  
175 as parts per million (ppm) unit were converted to g m<sup>-2</sup> h<sup>-1</sup> by the ideal gas law using measured temperature inside the chamber.  
176 If the flux was not yet stabilized at the beginning (first 4 datapoints) of the measurement, outliers were defined with Matlab  
177 isoutlier command resulting removal of 210 of total 23066 datapoints in 1564 flux measurements.

178 If the snow cover was thicker than 20 cm, a concentration snow gradient method as in Maljanen et al. (2003) was used to  
179 determine the GHG fluxes. A probe made of a steel pipe (Ø 3 mm), with a three-way valve and a plastic syringe, was used to  
180 sample 15 ml of air just above the snow cover, in the bottom of the snow cover and at every 10 cm in between in three  
181 replicate locations per plot. The gas was stored in the pre-evacuated vials and the concentrations were determined gas  
182 chromatographically.

183 Measurements for bare soil respiration were made in unvegetated subplots in 7/2019–12/2022. For willow, the large 60 × 60  
184 cm frames were used but for forage and set-aside we installed one sheet metal air ventilation pipe 27 cm in diameter and 30  
185 cm in length to the depth of 5–10 cm next to the opaque chamber collars in the 8 plots of grass and set-aside. All green  
186 vegetation within the chamber area was removed and root growth was limited by cutting around the chamber occasionally  
187 with a knife. For the measurements, the cylinders were closed with a cover equipped with a CO<sub>2</sub> sensor (GMP-343; Vaisala  
188 Oyj, Vantaa, Finland) and a small fan. One measurement lasted for one minute with a five second sampling rate.  
189 Measurements were taken about once in a week or two, more frequently in summer than in winter. In winters 2021 – 2022

190 and 2022 – 2023 this method was not used due to too high snow depth but measurements with the snow gradient method were  
191 utilized (Maljanen et al., 2003).

192

#### 193 **2.4. Flux modelling**

194 Gross photosynthesis (GP) can be determined as the difference of NEE and ER. Instantaneous GP was estimated for each  
195 measurement occasion by (equation 2),

196

$$197 \quad GP = NEE - ER \quad (2)$$

198

199 , where the full darkened transparent chamber measurement result (ER) is subtracted from the light-dependent flux (NEE)  
200 measured during the same day. Thus, we follow the sign convention with positive ER and negative GP values.

201 The gaps in GP and ER data between the measurement occasions were predicted using hourly timeseries of the ancillary data.  
202 Hourly time points for vegetation index, WTD and soil temperature and were acquired from the measured values by linear  
203 interpolation. Gaps in soil temperature were filled with the modified soil temperature model (Zheng et al., 1993) using the air  
204 temperature. Air temperature and PAR were assumed to be the same for all plots, whereas we used plot specific vegetation  
205 index and the soil temperature from the certain treatment. Hourly ER and GP were modelled using nonlinear regression  
206 (fitnlm function in MATLAB-2019b) for all 8 plots in forage and set-aside treatments. Empirical models were used for ER  
207 as in Lohila et al. (2003) and for GP as in Kandel et al. (2013). Instead of the phytomass indices used in the above publications,  
208 we used vegetation index formed according to the LAI and Canopeo measurements (index from 0 to 1) to describe the stage  
209 of the crop growth.

210 We used the following equation first defined by (Long and Hällgren, 1993) for GP to estimate empirical coefficients ( $A_{max}$   
211 and  $k$ ):

212

$$213 \quad GP = \frac{A_{Max} * PAR}{k + PAR} * VI * T_{Scale} \quad (3)$$

214

215 , where PAR is the measured photosynthetically active radiation ( $\mu\text{mol m}^{-2} \text{s}^{-1}$ ), VI is the vegetation index,  $A_{max}$  is the  
216 asymptotic maximum ( $\text{g CO}_2 \text{ m}^{-2} \text{ h}^{-1}$ ), and  $k$  is a half-saturation value ( $\mu\text{mol m}^{-2} \text{s}^{-1}$ ).  $T_{Scale}$  represents the temperature  
217 sensitivity of photosynthesis and follows the equation presented by (Raich et al., 1991):

218

$$219 \quad T_{Scale} = \frac{(T - T_{min})(T - T_{max})}{(T - T_{min})(T - T_{max}) - (T - T_{opt})^2} \quad (4)$$

220

221 , where  $T$  is the measured temperature, photosynthetically active minimum temperature  $T_{min}$  is  $-2 \text{ }^\circ\text{C}$ , maximum  $T_{max}$  is  $40 \text{ }^\circ\text{C}$   
222 and the optimum is  $20 \text{ }^\circ\text{C}$  as in (Kandel et al., 2013).

223 ER was estimated using data from the opaque and fully darkened transparent chambers. The empirical coefficients ( $R0_s$ ,  $R0_p$ ,  
224  $E0_s$  and  $b$ ) were estimated with a nonlinear regression model similarly as in the case of GP. Annual fluxes were computed as  
225 sum of the hourly fluxes with a trapezoidal method (trapz function in Matlab 2019b). ER consists of autotrophic ( $R_{auto}$ ), i.e.,  
226 plant respiration and heterotrophic ( $R_{hetero}$ ), i.e., soil respiration (LLOYD and TAYLOR, 1994) with extension of WTD as in  
227 (Karki et al., 2014):

228

$$229 \quad ER = R_{hetero} + R_{auto} \quad (5)$$

230

$$R_{hetero} = R0_s * \exp\left(E0_s \left(\frac{1}{56.02} - \frac{1}{T_{soil} + 46.02}\right)\right) + b * WTD \quad (6)$$

231  $R_{auto} = VI * R_{0p} * \exp \left( b_d \left( \frac{1}{10+273} - \frac{1}{T_{air}+273} \right) \right)$  (7)

232

233 , where  $T_{soil}$  is the measured soil temperature, VI is the vegetation index,  $T_{air}$  is the measured air temperature,  $R_{0s}$  is soil  
234 respiration at the reference temperature 10 °C ( $\text{g CO}_2 \text{ m}^{-2} \text{ h}^{-1}$ ),  $R_{0p}$  is plant respiration at the reference temperature at 10 °C  
235 ( $\text{g CO}_2 \text{ m}^{-2} \text{ h}^{-1}$ ), b is the effect of WTD,  $E_{0s}$  is ecosystem sensitivity and  $b_d$  ~~is~~ was the temperature dependence of dark  
236 respiration set to 5000 as in (Lohila et al., 2003). Bare soil respiration was estimated like ER but using only equation 6. The  
237 estimated parameters  $R_{0s}$ ,  $E_s$  and b and model R2 are shown in Table S3.

238

239

240

## 241 **2.5. Data processing and analysis**

242 For the transparent chamber measurements, the criterion  $R^2 > 0.9$  for the fitted linear assumption of flux measurements would  
243 exclude a large amount of data, especially with a small change in  $\text{CO}_2$ , leading to a biased dataset. Therefore, we decided to  
244 add the criterion  $S_{xy} < 2.3 \text{ g CO}_2 \text{ m}^{-2} \text{ h}^{-1}$  for dataset like in (Kutzbach et al., 2007) ( $S_{xy}$  is the standard deviation of the residuals  
245 and  $2.3 \text{ g m}^{-2} \text{ h}^{-1}$  is the 95% percentile of measurements). This procedure resulted in the removal of 59 values out of total  
246 1467 measurements. In the modelling phase, fitted values were examined, and outliers were removed to avoid distortion.  
247 Outliers were defined as observations with an absolute value of standardised residuals greater than three. In 2019, 3 out of  
248 260 GP values and 3 of 243 ER values were removed. In 2020, none of 200 GP values and 2 of 230 ER values were removed.  
249 2 out of 365 GP values and 4 of 247 ER values were removed in 2021 and 12 out of 583 GP values and 2 of 323 ER values  
250 were removed in 2022. The model's estimated parameters  $A_{max}$ , k of GP,  $R_{0s}$ ,  $R_{0p}$ ,  $E_s$  and b of ER and model correlations are  
251 shown in Table S2. The measured versus model predicted values of GP and ER are shown by treatments and years in Fig. S1.  
252 For bare soil respiration measurements in set-aside and forage, the same criteria were used as for transparent chamber ( $R^2 >$   
253  $0.9$  and  $S_{xy} < 95\%$ ) leading to a removal of 12 values of total 601. In bare soil measurements in midsummer 2022, there  
254 occurred 24 flux measurements (9 values in one plot, 0–5 in others) of total 147 values which were unexplained high (3–18  
255  $\text{g CO}_2 \text{ m}^{-2} \text{ h}^{-1}$ ). Values were of the same magnitude as values measured immediately after ploughing in (Honkanen et al.,  
256 2023). We decided to remove these values as outliers to avoid model distortion. Soil respiration of willow was defined with  
257 opaque chamber method and such outliers did not occur in these measurements. In modelling phase, outliers defined as  
258 observations with an absolute value of standardised residuals greater than three, were removed resulting removal of 13  
259 measurements of total 984 measurements (including all plots).

260 A linear regression model was fitted to calculate gas concentrations and the ideal gas law was used to solve the flux rate for  
261 every enclosure of the opaque chambers. Nonlinear responses of  $\text{CO}_2$  indicated a leaking chamber or other problem in the  
262 measurement and thus, if the  $R^2$  of  $\text{CO}_2$  was less than 0.9, also the results of  $\text{CH}_4$  and  $\text{N}_2\text{O}$  were discarded. In addition, sudden  
263 variations in  $\text{CH}_4$  fluxes due to ebullition were filtered by selecting only flux rates with the intercept between 1.5 and 2.4  
264 ppm. These criteria resulted to 176, 117 and 118 discarded values out of 1044 in the case of  $\text{CH}_4$ ,  $\text{CO}_2$  and  $\text{N}_2\text{O}$ , respectively.  
265 All data cleaning and processing was done with Matlab (The Math Works, Inc., MATLAB, version 2019b).

266

## 267 **2.6. GHG balance**

268 The annual net ecosystem carbon balance was constructed as the sum of the hourly values of NEE and yield data for each  
269 year in the case of forage and set-aside treatments. Modelling was used to fill the gaps between the measurement occasions  
270 to create a continuous series of hourly values. For willow, annual estimates of carbon loss in soil respiration were available  
271 from the chamber measurements from the unvegetated frames but as the willows were too high for the chambers their net  
272 production had to be estimated based on biomass accumulation during four years (Pacaldo et al., 2014). The presented net  
273 ecosystem carbon balance of willow is thus the sum of average annual  $\text{CO}_2\text{-C}$  from soil respiration and average annual amount



274 of carbon bound in the biomass during the four first cultivation years. The cumulative annual fluxes of CH<sub>4</sub> and N<sub>2</sub>O for each  
 275 management practice were calculated by interpolating the emissions between consecutive sampling days. Global warming  
 276 potentials 27 and 273 were used for CH<sub>4</sub> and N<sub>2</sub>O, respectively, to convert the results to CO<sub>2</sub> equivalents for the total GHG  
 277 balance (Forster et al. 2021).

278

## 279 2.7. Statistical analyses

280 Linear mixed models were used to find variables explaining variation in the gas fluxes. Crop, year, WTD and all their  
 281 interactions were denoted as fixed effects. Block and block × year were assumed to be independent and normally distributed  
 282 random effects. The most suitable covariance structure was chosen using Akaike's Information Criterion (AIC). The models  
 283 were fitted using the residual maximum likelihood (REML) method and degrees of freedom were estimated using the  
 284 Kenward-Roger method. The residuals were plotted against the fitted values and the normality of the residuals were checked  
 285 using boxplots. The data was log-~~or ln~~-transformed when needed to normalise the distributions. The method of Tukey-  
 286 Kramer was used for all pairwise comparisons of means with a significance level of 0.05. After the first model run with all  
 287 relevant variables the non-significant variables were removed one by one to find the most relevant effects. All statistical  
 288 analyses were performed using the SAS Enterprise Guide v7.1 (SAS Institute Inc., Cary, NC, USA).

289

## 290 3. Results

### 291 3.1 Climate and site variables

292 Annual mean temperature was 6.9, 6.0, 5.8 and 5.8 °C and annual precipitation 750, 600, 660, and 546 mm in 2019 – 2022,  
 293 respectively. Number of days with a snow-cover on the soil within each modelling year (April to March) was 13, 81, 108 and  
 294 118, respectively. The annual mean temperature during the study years was higher than the long-term average of 5.2°C in  
 295 1991–2020 (Jokinen et al., 2021). Two study years exhibited lower and two higher annual precipitation as compared to the  
 296 long-term mean of 621 mm. The WTD showed an increasing trend in time and high within-year variation (Fig. 1). The average  
 297 WTD was -54, -41, -39 and -27 cm in 2019–2022, respectively. WTD varied from -89 to -4, -77 to 2, -120 to 1.4 and -100 to  
 298 1.8 cm in 2019 – 2022, respectively.

299 The forage yields were 6.3±0.9, 8.9±0.7, 11±0.8 and 9.4±0.9 Mg DM ha<sup>-1</sup> in 2019-2022, respectively. There were two harvests  
 300 in 2020 and three in the other years. The plots were dominated by *Phleum pratense* and *Festuca pratensis* in 2021. The dry  
 301 mass yields of willow were 30±14 and 73±28 Mg DM ha<sup>-1</sup> in the harvests of February 2021 and 2023. Most of the C  
 302 accumulation occurred in the stem (59%), followed by stool (25%) and roots (9%) and foliage (7%) (Table 2). Vegetation of  
 303 the set-aside plots in 2021 was dominated by wild plants belonging to Families *Asteraceae*, *Cichoriaceae* and  
 304 *Caryophyllaceae*. Bog bilberry covered one percentage or less on each of the four replicate plots. The set-aside vegetation  
 305 had the highest species diversity, 19 vascular plants compared to 12 at willow plots and 9 at forage plots, the two latter  
 306 including crop plants.

307

308 **Table 2:** Four-year cumulative carbon balance of willow (±standard deviation). Negative sign indicates sequestered carbon  
 309 and positive sign released carbon to the atmosphere.

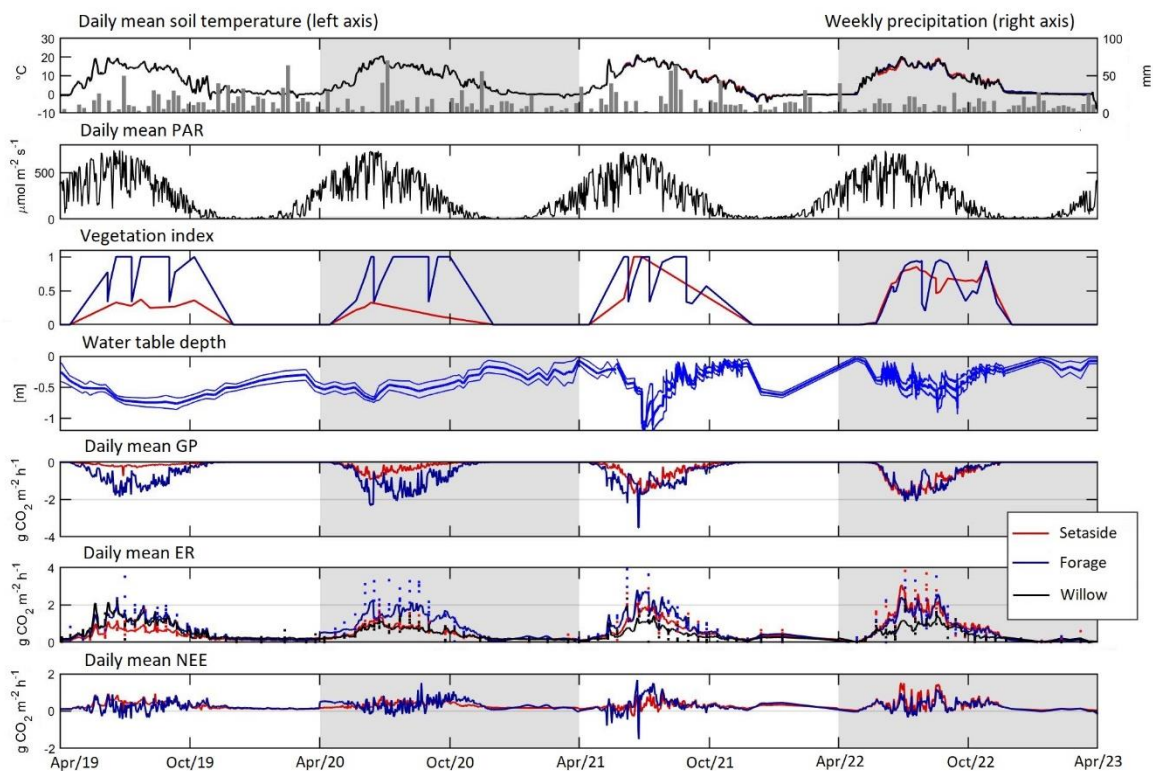
Component	Mg C ha <sup>-1</sup> 4 yrs <sup>-1</sup>	% of total
Stem (harvested)	-50.7±14.3	59
Foliage	-6.2±0.8	7
Aboveground stool	-12.6±3.2	15
Underground stool	-8.5±3.8	10
Coarse roots	-3.9±1.5	4
Fine roots	-4.6±0.6	5
Total sequestered carbon	-86.5±19.5	



Soil respiration	43.5±2.7
Net ecosystem exchange	-43.1±21.1
Net ecosystem carbon balance	7.6±7.7

310

311



312

313 **Figure 1:** Daily mean of soil temperature and precipitation, photosynthetically active radiation (PAR),  
 314 water table depth (site mean±std), gross photosynthesis-, measured (dots) and model predicted (line) ecosystem respiration  
 315 (soil respiration for willow) -and net ecosystem exchange. Annual modelling periods (Apr - Mar) are marked with light grey  
 316 or white background.

317

318

### 319 3.2. Carbon balance

320 Model predicted maximum hourly GP was -0.7, -3.2, -4.3 and -4.8 g CO<sub>2</sub> m<sup>-2</sup> h<sup>-1</sup> in the set-aside in 2019 – 2020, and -3.9, -  
 321 5.9, -4.3 and -4.8 g CO<sub>2</sub> m<sup>-2</sup> h<sup>-1</sup> in the forage plots in 2019–2022, respectively (Fig. S1). Maximum measured GP value was -  
 322 1.1, -2.4, -3.4 and -4.5 g CO<sub>2</sub> m<sup>-2</sup> h<sup>-1</sup> for set-aside and -3.4, -6.2, -4.8 and -4.2 g CO<sub>2</sub> m<sup>-2</sup> h<sup>-1</sup> for forage in 2019–2020,  
 323 respectively. Annual values of GP varied from -9.3 to -12 Mg CO<sub>2</sub>-C ha<sup>-1</sup> yr<sup>-1</sup> in the forage and from -1.5 to -10 Mg CO<sub>2</sub>-C  
 324 ha<sup>-1</sup> yr<sup>-1</sup> in the set-aside treatment (Table 3). The -WTD explained variation in GP variables initially included in the analysis  
 325 were annual mean WTD, crop type and year as main effects and all their interactions. Finally, only crop, year and their  
 326 interaction were left in the model (Table S4). Inclusion of WTD did not result in a meaningful estimate as both the productivity  
 327 of especially the set-aside established in 2019 and the WTD increased with years, and the observed change in GP did not in  
 328 reality increase with WTD but with time. F(p=0.011), but forage and set-aside treatments did not differ  
 329 (p<0.001), there was an increasing trend in productivity from 2019–2022 (p=0.0009) and the differences between the crop  
 330 types were highest in 2019–2021 (p<0.001). However, there was an interaction between the treatment and WTD indicating  
 331 that WTD affected GP of the set-aside treatment more than that of the forage (p=0.008).

B32

B33

334  
335  
336  
337  
338  
339  
340  
341

**Table 3:** The estimated annual sums ( $\pm$ standard deviation) of gross photosynthesis (GP), ecosystem respiration (ER), net ecosystem exchange (NEE), carbon exported in the harvested yield, net ecosystem carbon balance (NECB), N<sub>2</sub>O and CH<sub>4</sub> effluxes and the total emissions (global warming potential of one hundred years; GWP-100) with either NEE or NECB representing CO<sub>2</sub> emissions in the forage and set-aside plots, and selected data for willow. Significant differences ( $p < 0.05$ ) between treatments within a year are denoted with different letters ( $n=4$ ).

Year	Variable and unit	Forage	Set-aside	Willow <sup>a</sup>
2019	GP Mg CO <sub>2</sub> -C ha <sup>-1</sup>	-9.31 $\pm$ 0.75a	-1.48 $\pm$ 0.32b	
	ER Mg CO <sub>2</sub> -C ha <sup>-1</sup>	14.4 $\pm$ 2.17a	8.25 $\pm$ 2.40b	
	NEE Mg CO <sub>2</sub> -C ha <sup>-1</sup>	5.08 $\pm$ 1.80	6.77 $\pm$ 2.41	
	C in yield Mg C ha <sup>-1</sup>	3.17 $\pm$ 0.49	0	
	NECB Mg C ha <sup>-1</sup>	8.25 $\pm$ 2.13	6.77 $\pm$ 2.41	
	Soil respiration Mg CO <sub>2</sub> -C ha <sup>-1</sup>	12.8 $\pm$ 4.99	11.4 $\pm$ 1.82	14.8 $\pm$ 0.76
	N <sub>2</sub> O-N kg ha <sup>-1</sup>	11.9 $\pm$ 7.60a	32.6 $\pm$ 12.1b	17.4 $\pm$ 10.3
	CH <sub>4</sub> -C kg ha <sup>-1</sup>	-0.28 $\pm$ 0.75	-1.00 $\pm$ 0.73	-1.64 $\pm$ 0.26
	GWP <sub>100</sub> Mg CO <sub>2</sub> eq ha <sup>-1</sup> (NEE) <sup>b</sup>	23.7 $\pm$ 5.67	38.8 $\pm$ 19.8	
	GWP <sub>100</sub> Mg CO <sub>2</sub> eq ha <sup>-1</sup> (NECB) <sup>c</sup>	35.3 $\pm$ 6.86	38.8 $\pm$ 19.8	
2020	GP Mg CO <sub>2</sub> -C ha <sup>-1</sup>	-11.7 $\pm$ 1.17a	-3.57 $\pm$ 0.46b	
	ER Mg CO <sub>2</sub> -C ha <sup>-1</sup>	19.3 $\pm$ 1.85a	10.6 $\pm$ 1.49b	
	NEE Mg CO <sub>2</sub> -C ha <sup>-1</sup>	7.64 $\pm$ 1.75	7.05 $\pm$ 1.12	
	C in yield Mg C ha <sup>-1</sup>	3.35 $\pm$ 1.28	0	
	NECB Mg C ha <sup>-1</sup>	11.0 $\pm$ 2.02	7.05 $\pm$ 1.12	
	Soil respiration Mg CO <sub>2</sub> -C ha <sup>-1</sup>	9.09 $\pm$ 4.86	10.6 $\pm$ 0.97	10.0 $\pm$ 0.79
	N <sub>2</sub> O-N kg ha <sup>-1</sup>	6.26 $\pm$ 3.39	6.59 $\pm$ 2.97	4.61 $\pm$ 2.99
	CH <sub>4</sub> -C kg ha <sup>-1</sup>	-0.36 $\pm$ 0.40	-1.01 $\pm$ 0.56	-1.13 $\pm$ 0.33
	GWP <sub>100</sub> Mg CO <sub>2</sub> eq ha <sup>-1</sup> (NEE)	30.4 $\pm$ 7.64	28.7 $\pm$ 3.73	
	GWP <sub>100</sub> Mg CO <sub>2</sub> eq ha <sup>-1</sup> (NECB)	42.6 $\pm$ 8.69	28.7 $\pm$ 3.73	
2021	GP Mg CO <sub>2</sub> -C ha <sup>-1</sup>	-9.46 $\pm$ 1.20a	-6.34 $\pm$ 0.68b	
	ER Mg CO <sub>2</sub> -C ha <sup>-1</sup>	17.4 $\pm$ 1.40a	13.5 $\pm$ 1.82b	
	NEE Mg CO <sub>2</sub> -C ha <sup>-1</sup>	7.95 $\pm$ 2.16	7.12 $\pm$ 2.16	
	C in yield Mg C ha <sup>-1</sup>	5.54 $\pm$ 0.46	0	
	NECB Mg C ha <sup>-1</sup>	13.5 $\pm$ 1.88a	7.12 $\pm$ 2.16b	
	Soil respiration Mg CO <sub>2</sub> -C ha <sup>-1</sup>	7.82 $\pm$ 2.30	11.5 $\pm$ 2.44	8.99 $\pm$ 2.70
	N <sub>2</sub> O-N kg ha <sup>-1</sup>	6.49 $\pm$ 3.88a	2.18 $\pm$ 0.24b	5.75 $\pm$ 6.25
	CH <sub>4</sub> -C kg ha <sup>-1</sup>	7.92 $\pm$ 12.7	0.58 $\pm$ 1.87	3.89 $\pm$ 6.12
	GWP <sub>100</sub> Mg CO <sub>2</sub> eq ha <sup>-1</sup> (NEE)	32.2 $\pm$ 8.16	27.1 $\pm$ 8.03	
	GWP <sub>100</sub> Mg CO <sub>2</sub> eq ha <sup>-1</sup> (NECB)	52.2 $\pm$ 6.93	27.1 $\pm$ 8.03	
2022	GP Mg CO <sub>2</sub> -C ha <sup>-1</sup>	-9.34 $\pm$ 2.13	-9.65 $\pm$ 2.08	
	ER Mg CO <sub>2</sub> -C ha <sup>-1</sup>	14.4 $\pm$ 3.29	16.5 $\pm$ 3.21	
	NEE Mg CO <sub>2</sub> -C ha <sup>-1</sup>	5.10 $\pm$ 1.15	6.82 $\pm$ 1.15	
	C in yield Mg C ha <sup>-1</sup>	4.72 $\pm$ 0.50	0	
	NECB Mg C ha <sup>-1</sup>	5.46 $\pm$ 6.37	6.82 $\pm$ 1.15	
	Soil respiration Mg CO <sub>2</sub> -C ha <sup>-1</sup>	8.40 $\pm$ 1.48	15.0 $\pm$ 5.32	9.70 $\pm$ 2.3
	N <sub>2</sub> O-N kg ha <sup>-1</sup>	9.54 $\pm$ 4.49a	3.07 $\pm$ 0.86b	1.69 $\pm$ 1.10b
	CH <sub>4</sub> -C kg ha <sup>-1</sup>	7.74 $\pm$ 0.59	11.3 $\pm$ 7.72	10.9 $\pm$ 12.9
	GWP <sub>100</sub> Mg CO <sub>2</sub> eq ha <sup>-1</sup> (NEE)	22.9 $\pm$ 3.34	26.6 $\pm$ 4.61	
	GWP <sub>100</sub> Mg CO <sub>2</sub> eq ha <sup>-1</sup> (NECB)	43.3 $\pm$ 3.18	26.6 $\pm$ 4.61	

342 <sup>a</sup>All components of the carbon balance are not available for willow, see chapter 2.6, <sup>b</sup>With NEE representing CO<sub>2</sub>, <sup>c</sup>With  
343 NEBC representing CO<sub>2</sub>

344  
345 Modelled maximum hourly ER was 2.4, 2.3, 3.0 and 4.7 g CO<sub>2</sub> m<sup>-2</sup> h<sup>-1</sup> in the set-aside and 3.5, 3.4, 4.8 and 4.5 g CO<sub>2</sub>-C m<sup>-2</sup>  
346 h<sup>-1</sup> in the forage plots (Fig. S1). Measured maximum ER with the opaque chamber method was 1.7, 2.0, 2.9 and 4.6 g CO<sub>2</sub>-C  
347 m<sup>-2</sup> h<sup>-1</sup> for the set-aside and 3.5, 4.2, 4.0 and 4.8 g CO<sub>2</sub>-C m<sup>-2</sup> h<sup>-1</sup> for forage. Annual ER varied from 14 to 19 Mg CO<sub>2</sub>-C ha<sup>-1</sup>  
348 yr<sup>-1</sup> in the forage and from 8 to 17 Mg CO<sub>2</sub>-C ha<sup>-1</sup> yr<sup>-1</sup> in set-aside treatment (Table 3). Variables initially included in the  
349 analysis were annual mean WTD, crop type and year as main effects as well as their interactions. WTD did not well explain  
350 the variation in the annual ER estimate, likely for the same reason as for GP as plant respiration is related to the biomass of  
351 the vegetation, which increased during the experimental years. (p=0.062), and the forage and set-aside treatments did not  
352 differ significantly. The best model was based on the crop type and year as main effects, and their interactions (Table S4). In  
353 this model, crop type explained ER well, ER increased in time, and ER increased between years more in forage than set-aside.  
354 However, there was an interaction between the treatment and WTD indicating that WTD affected ER of the set-aside treatment  
355 more than that of the forage (p=0.032).

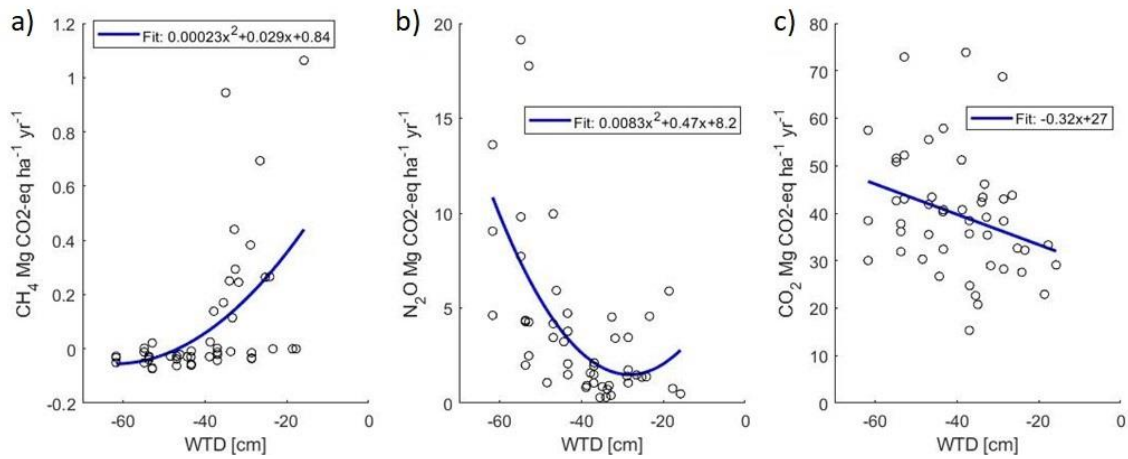
356 Hourly model-predicted NEE varied from -2.9 to 3.7 g CO<sub>2</sub> m<sup>-2</sup> h<sup>-1</sup> in the set-aside and from -4.6 to 3.7 g CO<sub>2</sub> m<sup>-2</sup> h<sup>-1</sup> in the  
357 forage treatment (results not shown). There were 29, 28, 16 and 47 days annually with negative daily NEE in the forage plots  
358 during the study years, respectively, and fewer such days (1, 0, 9 and 6) in the set-aside plots in 2019–2022 (Fig. 1). The  
359 cumulative annual balance ranged from 5.1 to 8.0 Mg CO<sub>2</sub>-C ha<sup>-1</sup> yr<sup>-1</sup> in the forage and from 6.8 to 7.1 Mg CO<sub>2</sub>-C ha<sup>-1</sup> yr<sup>-1</sup> in  
360 the set-aside treatment (Table 3) and the treatments did not differ statistically. The net ecosystem carbon balance (NECB)  
361 that accounts the amount of carbon exported in the harvested yield varied from 5.5 to 13.5 Mg CO<sub>2</sub>-C ha<sup>-1</sup> yr<sup>-1</sup> in the forage  
362 treatment and were equal to NEE in the set-aside treatment (Table 3). The NECB values differed statistically between the  
363 forage and set-aside treatments across all years (p>0.001) and inclusion of additional effects in the analysis did not improve  
364 the model (Table S4).

365 Annual sum of respiration varied from 8 to 15 Mg CO<sub>2</sub>-C ha<sup>-1</sup> yr<sup>-1</sup> in the different treatments and years (Table 3). The  
366 proportion of soil respiration of the total ecosystem respiration varied from 45 to 90% in the forage plots and from 85 to 100%  
367 in the set-aside plots in 2019–2022. In the set-aside plots, estimated annual bare soil respiration exceeded the estimated ER  
368 in all plots in 2019, two plots in 2020 and one plots in 2021 and 2022 and those values were not used in the above calculation,  
369 and thus it is assumed that total respiration constituted only of soil respiration in 2019. Annual cumulative soil respiration  
370 was explained by ~~the~~ WTD (Fig. 2; p=0.053) and crop type (p=0.033) so that forage and set-aside treatments were  
371 significantly different in the whole dataset and respiration increased in the order forage<willow<set-aside (Fig. S4; Table S4).

372 Plots of the bare soil respiration in relation to WTD and temperature show that there is a clear trend of decreasing respiration  
373 with raising WTD (Fig. S2). Three individual curves indicate a contrasting trend, but these three estimations are based on a  
374 small number of measurement results. Based on all annual estimates of soil respiration, a 0.1 m raise in WTD reduces  
375 respiration by 0.87 Mg CO<sub>2</sub>-C ha<sup>-1</sup> yr<sup>-1</sup>.

376 The cumulative total amount of C in the above and below ground willow biomass was 86.5 Mg C ha<sup>-1</sup> during the four study  
377 years (Table 2). About 40% of the carbon in the biomass was left at the site after harvest, and soil respiration amounted to  
378 43.5 Mg ha<sup>-1</sup>, leading to a strongly negative cumulative NEE of -43 Mg ha<sup>-1</sup>. Carbon export in the harvest changed the net  
379 balance to net loss of 7.6 Mg, corresponding to an average annual CO<sub>2</sub> rate of 7 Mg of CO<sub>2</sub>.

380



381

382 **Fig. 2.** Plot-wise mean annual fluxes of CH<sub>4</sub> (a), N<sub>2</sub>O (b) and soil respiration (c) (CO<sub>2</sub> eq.) as related to the mean annual  
 383 WTD.

384

385

386

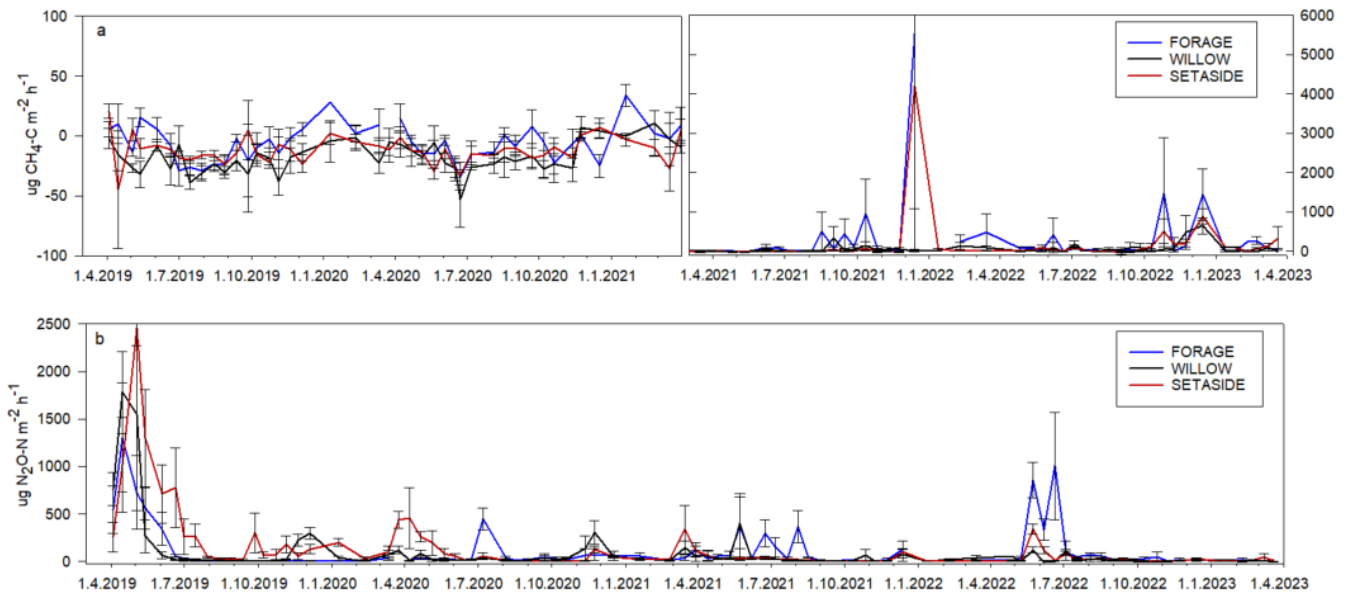
### 387 3.3. CH<sub>4</sub> fluxes

388 Hourly fluxes of CH<sub>4</sub> varied between -50 and 30 μg CH<sub>4</sub>-C m<sup>-2</sup> h<sup>-1</sup> during the first half of the experimental period (Fig. 3). In  
 389 conjunction with the raise in the WTD the values the hourly fluxes increased and varied between -40 and 900 μg m<sup>-2</sup> h<sup>-1</sup>  
 390 during the latter half of the period. The annual flux of CH<sub>4</sub> varied from -1.6 to 11 kg CH<sub>4</sub>-C ha<sup>-1</sup> yr<sup>-1</sup> with an increasing trend  
 391 towards the end of the measurement period (Table 3; Fig. S3). When the mean annual WTD was below 40 cm the soil was  
 392 mainly consuming CH<sub>4</sub>, but the consumption tended to change to emissions as the WTD raised (Fig. 2).— Variation in the  
 393 annual cumulative fluxes of each plot was explained by the WTD (p=0.01549) but not by crop (Table S4). The increasing  
 394 trend between years 2019–2022 was also shown in the mixed model analysis—~~or~~ as year had a significant effect (p=0.0003)  
 395 and the effect of WTD decreased with time (years). ~~When the mean annual WTD was below 40 cm the soil was mainly~~  
 396 ~~consuming CH<sub>4</sub>, but the consumption tended to change to emissions as the WTD raised (Fig. 2).~~

397

### 398 3.4. N<sub>2</sub>O fluxes

399 Hourly fluxes of N<sub>2</sub>O varied between -3 and 2500 μg N<sub>2</sub>O-N m<sup>-2</sup> h<sup>-1</sup> during the four years with the highest emissions during  
 400 the first four months (Fig. 3). Annual fluxes of N<sub>2</sub>O varied from 1.7 to 33 kg N<sub>2</sub>O-N ha<sup>-1</sup> yr<sup>-1</sup> (Table 3). The emissions declined  
 401 in time (Fig. S3) especially in the case of set-aside and willow whereas those of forage did not show such a trend (Table 3).  
 402 WTD explained variation in N<sub>2</sub>O fluxes well (p=0.01527) (Fig. 2; Table S4). There were some interactions of year and crop,  
 403 but the crop type did not affect N<sub>2</sub>O emissions systematically between years. Annual N<sub>2</sub>O fluxes of the forage and willow  
 404 treatments differed in the whole timeseries (p=0.0269).  
 405



406

407

408

**Fig. 3.** Fluxes of CH<sub>4</sub> (a) and N<sub>2</sub>O (b) in 2019-2023. The error bars denote standard error. Note the different scale in the y-axis of (a) for the latter half of the period.

409

410

411

### 3.5. Global warming potential

412

413

414

415

416

417

The total emissions expressed as CO<sub>2</sub> equivalents ranged from 23 to 39 Mg ha<sup>-1</sup> yr<sup>-1</sup> with NEE as the CO<sub>2</sub> component and from 27 to 52 Mg with the C export in harvest taken into account in the forage and set-aside treatments (Table 3). For willow, the annual NECB cannot be calculated but based on the four-year estimate on carbon binding in the biomass and carbon exported in the harvest divided to a single year, together with the average annual soil respiration and N<sub>2</sub>O and CH<sub>4</sub> fluxes, the average annual climate impact of willow cultivation was 10.2 Mg ha<sup>-1</sup> yr<sup>-1</sup>.

418

## 4. Discussion

419

420

421

422

423

424

425

426

427

428

429

430

431

432

433

434

435

NEE values of 5–8 Mg C ha<sup>-1</sup> per year in the forage plots were of the same magnitude as values reported for grass cultivation in northern Europe (Maljanen et al., 2010). They were, however, 6–10 times higher than NEE reported for year 2002 in a nearby field (Lohila et al., 2004), highlighting the spatial and temporal variation in soil emissions. During the first two years of the experiment, the CH<sub>4</sub> fluxes of the forage plots were negative indicating net consumption of CH<sub>4</sub> by the soil microorganism. The CH<sub>4</sub> oxidation rates were generally higher than average values reported from Nordic cultivated peat soils which have shown net positive values for grass fields (Maljanen et al., 2007, 2010). There was a change from negative fluxes of CH<sub>4</sub> to relatively high emissions after the annual mean water table rose above -40 cm during the two latter years of the experiment. However, compared to rewetted agricultural sites in the temperate zone, the values of ca. 8 kg CH<sub>4</sub>-C per hectare were clearly lower than the average of 180 kg CH<sub>4</sub>-C ha<sup>-1</sup> yr<sup>-1</sup> found in temperate paludiculture-like grassland ecosystems (Bianchi et al., 2021). The N<sub>2</sub>O emissions ranging from 6 to 12 kg N per hectare annually were typical for northern European grass fields on organic soils as they were within the 95% confidence interval of the reported values from temperate and boreal regions (Hiraishi et al., 2014). After the high emission peak in the beginning of the experiment there were only short-term peaks after fertilisation. One of them was especially high and long-lasting and likely induced by heavy rainfall after a long dry period coinciding with fertilisation in May-June 2022. It is typical that high peaks after fertilisation occur when fertilisation is followed by rainfall (Dobbie et al., 1999), and fertiliser-induced peaks may be totally absent if there is no coinciding rainfall (Beetz et al., 2013). The set-aside plots with slowly evolving vegetation had clearly lower GP than the forage plots during the three first years. However, also the ER was lower in the set-aside, and the resulting NEE was of the

436 same magnitude in both treatments. Because there was no biomass export from the set-aside the NECB was lower than in the  
437 forage treatment in most years. The modelled NEE values were about double compared to long-term abandoned croplands in  
438 the Nordic countries (Maljanen et al., 2010) but in our study the plots did not represent similar ecosystems as they were  
439 “abandoned” only for a short period. N<sub>2</sub>O fluxes of the set-aside plots were extremely high in 2019 compared to results of  
440 previous studies on cultivated peat soils in Nordic countries (Maljanen et al., 2010). As the “set-aside” was fertilised and  
441 unsuccessfully planted with bog bilberry, the high emissions were likely due to abundant free mineral nitrogen in the absence  
442 of plant nutrient uptake. As the berry plants did not thrive, the soil was bare for a long period and the N<sub>2</sub>O emissions remained  
443 higher than in the other treatments throughout the summer. Such conditions were prevailing also in a similar bare fallow  
444 treatment at a nearby site in 2000-2002, yielding average N<sub>2</sub>O emissions of 25 kg N ha<sup>-1</sup> yr<sup>-1</sup> (Regina et al., 2004). During the  
445 second year, the emissions lowered but as the plots were fertilised also in 2020, they still exhibited as high emissions as the  
446 forage plots. During the last two years the N<sub>2</sub>O emissions were at a notably low level which likely resulted from ceasing of  
447 fertilisation and a slightly higher WTD leading to less peat being exposed to aerobic conditions. Raising the WTD has been  
448 found to diminish N<sub>2</sub>O emissions in several studies (van Beek et al., 2010; Leppelt et al., 2014).

449  
450  
451 Willow grew well at this site and the mean annual yields were in the higher end of the range 4-16 Mg ha<sup>-1</sup> estimated for  
452 northern climate conditions (Viherä-Aarnio et al., 2022). Carbon lost in soil respiration was lower than the amount sequestered  
453 in the willow biomass in all years except in 2019, leading to highly negative NEE during the whole rotation. However, the  
454 amount of carbon exported in harvest exceeded the NEE and the yielding NECB indicated net loss of carbon to the  
455 atmosphere. Although the average annual NECB calculated from the four-year carbon balance (1.9 Mg C ha<sup>-1</sup> yr<sup>-1</sup>) was low  
456 compared to the forage or set-aside treatments, it still indicated a climate-warming end result in short-rotation cropping of  
457 willow on peat soil. It is possible to achieve a net positive NEBC in willow cultivation on mineral soils (Harris et al., 2017;  
458 Morrison et al., 2019) but in peatlands the high rate of soil respiration inevitably reduces this potential (Kasimir et al., 2018).

459  
460 The target WTD was not reached for most of the time likely because there was unexcepted lateral water outflow from the  
461 site. Our strategy of raising the WTD at a limited area within a field parcel was thus not successful. The larger the area where  
462 the water outflow is restricted, the better the result likely is, and catchment level water management planning is often  
463 recommended for the best results (Mitsch and Wilson, 1996; Pasquet et al., 2015).

464 The annual emissions can be compared to a well-drained cereal site (oats; mean WTD 68 cm) on the same field (Honkanen  
465 et al., 2023), as the distance between these two experiments was just about 20 m. In 2020, when similar measurements were  
466 conducted in both experiments, the total GHG balance (GWP100 with harvest) was 29 Mg in the set-aside and 43 Mg in the  
467 forage treatment while it was 39 Mg CO<sub>2</sub>-eq. in the conventionally managed cereal plots. As the comparable number for  
468 willow was 10 Mg in the willow treatment, it can be argued that the set-aside and willow cultivation with a moderate raise of  
469 WTD were better management options than cultivation of annual crops with a typical drainage depth. It was also clear that  
470 willow had the best GHG balance of these three management options, which is in agreement with findings of grassland and  
471 willow cropping in southern England (Harris et al., 2017). However, the total emissions were still relatively high suggesting  
472 that this kind of moderately wet management is not an efficient climate mitigation measure. This was also shown by the  
473 modelling results of (Kasimir et al., 2018) concluding that fully rewetted peatland had the most favourable carbon balance  
474 and less emissions from soil in a comparison of four different peatland management scenarios. However, management  
475 decisions, like cutting height also play a role in determining the final carbon balance in short-rotation cropping (Berhongaray  
476 et al., 2017).

477 Set-aside is a relevant management option to study because many cultivated peat fields end up as uncultivated plots when  
478 their drainage system degrades, and the landowner finds them too wet for cultivation. The annual total emissions were lower



479 in the set-aside plots compared to the forage in 2020 and 2021, and also in 2022 if the carbon exported in harvest is taken into  
480 account. However, they were not especially low as compared to cultivated peat soils in general. Thus, leaving cultivated peat  
481 soils uncultivated without active rewetting is not desirable form of land management as these sites drift out from food  
482 production, but the GHG emissions can remain high. A recent Swedish study also found that setting aside did not reduce  
483 GHG emissions from a drained peat soil (Keck et al., 2024)

484 Our set-aside plots were actually intended to be vegetated by bog bilberry, a native mire plant that could become a novel  
485 antioxidant-rich ingredient for food (Lätti et al., 2010) or pharmaceutical (Esposito et al., 2019) industries. However, we soon  
486 noticed that the seedlings did not grow roots indicating that formerly agriculturally cultivated peat was not a suitable substrate  
487 for this plant. As the nutrient content of the topsoil did not show large deviations from the reported ranges supporting the  
488 growth of bog bilberry (Jacquemart, 1996), it is likely that the pH of 5.4 at our site was too high. Bog bilberry is usually found  
489 in soils with pH below 5. However, in recent trials it has been successfully grown on Chinese farmlands with pH 5–6 but low  
490 pH improved the growth also there (Duan et al., 2022).

491  
492 There are usually high uncertainties in the GHG measurements, and this is especially true regarding the combination of  
493 methods chosen for the willow treatment. The carbon balance of willow was determined using a combination of the pool-  
494 based and flux-based methods, which can differ by several magnitudes (Berhongaray et al., 2017). The most reliable method  
495 for measuring the carbon balance of willow stands is likely the eddy covariance method, which is not feasible in experiments  
496 with small plots. Part of the uncertainty also arises from the simplicity of the models. For example, soil respiration was  
497 modelled only based on soil temperature and WTD, although it can be affected also e.g. by changes in microbial community  
498 composition or activity (Yang et al. 2022) and soil moisture which does not always well follow changes in WTD (Smith et  
499 al. 2018). Estimating vegetation cover using measured LAI is also problematic, as it reflects weakly the amount of active  
500 chlorophyll (Delegido et al., 2015; Gregersen et al., 2013). It is especially difficult to assess active vegetation at the beginning  
501 and end of the growing season. However, the influence on the annual balance is minor due to low temperature and radiation  
502 at that time. With the Canopeo application, the models were significantly better as it was possible to determine the green leaf  
503 area better than with the previously used LAI measurement with the SunScan instrument. The measurement results of PAR  
504 values feature uncertainties due to abrupt changes in cloudiness or fogging and dirt on the plexiglass. Due to technical  
505 problems, FMI data and another PAR sensor was used to fill the gaps in the PAR measurements especially in 2021. The  
506 plexiglass surfaces were kept as clean as possible, fogging was kept low by using a short measurement time, and clear sky  
507 conditions were preferred which should reduce the uncertainty occurred in measurements. Model predicted soil temperature  
508 in gap filling may cause some error, but the filled gaps were not long, and the error was mostly diurnal with low significance  
509 for the annual balances. Regarding biweekly N<sub>2</sub>O and CH<sub>4</sub> measurements, there is a high risk of missing short-term peaks,  
510 for example due to freeze-thaw cycles (Lammirato et al., 2021). Also, if the measurements hit peaks, the emissions may be  
511 overestimated due to interpolation of the gaps in the data particularly during times with infrequent measurements.

## 512 513 **5 Conclusions**

514 This study gave valuable insights to the practical implementation and climate mitigation potential of three management  
515 options relevant for cultivated peatlands with raised WTD: forage, willow and set-aside. The results indicate that wet  
516 management of cultivated peat soils considerably reduces the soil respiration and N<sub>2</sub>O emissions. Significant counteracting  
517 effect of increased CH<sub>4</sub> emissions are avoided as long as the WTD does not rise close to the soil surface. However, compared  
518 to full rewetting, partial rewetting remains a compromise solution to climate warming as it is likely that the peat layer will  
519 eventually be lost. It is important to develop incentives to inundate large, connected peatland areas to ensure water availability  
520 and maintenance of high enough water table for efficient control of peat decomposition.

521

522 **Authorship contributions.** KL and HK designed the experiment. JH, HH, SS and TL developed the methodology. HK and  
523 TL planned, supervised and partly conducted the field work. KL, HH and HK analysed and visualised the data. KL and HH  
524 wrote the original manuscript. All authors were involved in revising the text.

525

526 **Data availability.** The data will be available in Zenodo two years after publication.

527

528 **Competing interests.** The contact author has declared that none of the authors has any competing interests.

529

530 **Acknowledgements.** The authors are grateful to the technical staff of Natural Resources Institute Finland for skilled work in  
531 the field and laboratory.

532

533 **Financial support.** This study was part of the project SOMPA (Novel soil management practices – key for sustainable  
534 bioeconomy and climate change mitigation), funded by the Strategic Research Council at the Research Council of Finland,  
535 grant No 312912 and INSURE (Indicators for successful carbon sequestration and greenhouse gas mitigation by rewetting  
536 cultivated peat soils) subproject of the EJP Soil project that has received funding from the European Union’s Horizon 2020  
537 research and innovation programme under grant agreement No 862695.

538

539

540

541

## 542 **References**

543 Aparicio, N., Villegas, D., Casadesus, J., Araus, J. L., and Royo, C.: Spectral Vegetation Indices as Nondestructive Tools  
544 for Determining Durum Wheat Yield, *Agron. J.*, 92, 83–91, <https://doi.org/10.2134/agronj2000.92183x>, 2000.

545 van Beek, C. L., Pleijter, M., Jacobs, C. M. J., Velthof, G. L., van Groenigen, J. W., and Kuikman, P. J.: Emissions of N<sub>2</sub>O  
546 from fertilized and grazed grassland on organic soil in relation to groundwater level, *Nutr. Cycl. Agroecosystems*, 86, 331–  
547 340, <https://doi.org/10.1007/s10705-009-9295-2>, 2010.

548 Beetz, S., Liebersbach, H., Glatzel, S., Jurasinski, G., Buczko, U., and Hoeper, H.: Effects of land use intensity on the full  
549 greenhouse gas balance in an Atlantic peat bog, *Biogeosciences*, 10, 1067–1082, <https://doi.org/10.5194/bg-10-1067-2013>,  
550 2013.

551 Berhongaray, G., Verlinden, M. S., Broeckx, L. S., Janssens, I. A., and Ceulemans, R.: Soil carbon and belowground carbon  
552 balance of a short-rotation coppice: assessments from three different approaches, *GCB Bioenergy*, 9, 299–313,  
553 <https://doi.org/10.1111/gcbb.12369>, 2017.

554 Bianchi, A., Larmola, T., Kekkonen, H., Saarnio, S., and Lang, K.: Review of Greenhouse Gas Emissions from Rewetted  
555 Agricultural Soils, *WETLANDS*, 41, 108, <https://doi.org/10.1007/s13157-021-01507-5>, 2021.

556 Bockermann, C., Eickenscheidt, T., and Droesler, M.: Adaptation of fen peatlands to climate change: rewetting and  
557 management shift can reduce greenhouse gas emissions and offset climate warming effects, *BIOGEOCHEMISTRY*,  
558 <https://doi.org/10.1007/s10533-023-01113-z>, 2024.

559 Boonman, C. C. F., Heuts, T. S., Vroom, R. J. E., Geurts, J. J. M., and Fritz, C.: Wetland plant development overrides  
560 nitrogen effects on initial methane emissions after peat rewetting, *Aquat. Bot.*, 184, 103598,  
561 <https://doi.org/10.1016/j.aquabot.2022.103598>, 2023.

562 Delegido, J., Verrelst, J., Rivera, J. P., Ruiz-Verdú, A., and Moreno, J.: Brown and *green* LAI mapping through spectral  
563 indices, *Int. J. Appl. Earth Obs. Geoinformation*, 35, 350–358, <https://doi.org/10.1016/j.jag.2014.10.001>, 2015.

564 Dobbie, K. E., McTaggart, I. P., and Smith, K. A.: Nitrous oxide emissions from intensive agricultural systems: Variations  
565 between crops and seasons, key driving variables, and mean emission factors, *J. Geophys. Res. Atmospheres*, 104, 26891–  
566 26899, <https://doi.org/10.1029/1999JD900378>, 1999.

- 567 Duan, Y., Guo, B., Zhang, L., Li, J., Li, S., Zhao, W., Yang, G., Zhou, S., Zhou, C., Song, P., Li, P., Fang, L., Hou, S., Shi,  
568 D., Zhao, H., and Guo, P.: Interactive climate-soil forces shape the spatial distribution of foliar N:P stoichiometry in  
569 *Vaccinium uliginosum* planted in agroforests of Northeast China, *Front. Ecol. Evol.*, 10,  
570 <https://doi.org/10.3389/fevo.2022.1065680>, 2022.
- 571 Esposito, D., Overall, J., and Grace, M. H.: Alaskan Berry Extracts Promote Dermal Wound Repair Through Modulation of  
572 Bioenergetics and Integrin Signaling, *Front. Pharmacol.*, 10, <https://doi.org/10.3389/fphar.2019.01058>, 2019.
- 573 Evans, C. D., Peacock, M., Baird, A. J., Artz, R. R. E., Burden, A., Callaghan, N., Chapman, P. J., Cooper, H. M., Coyle,  
574 M., Craig, E., Cumming, A., Dixon, S., Gauci, V., Grayson, R. P., Helfter, C., Heppell, C. M., Holden, J., Jones, D. L.,  
575 Kaduk, J., Levy, P., Matthews, R., McNamara, N. P., Misselbrook, T., Oakley, S., Page, S. E., Rayment, M., Ridley, L. M.,  
576 Stanley, K. M., Williamson, J. L., Worrall, F., and Morrison, R.: Overriding water table control on managed peatland  
577 greenhouse gas emissions, *Nature*, <https://doi.org/10.1038/s41586-021-03523-1>, 2021.
- 578 [FMI 2024. Finnish Meteorological Institute open data on weather monitoring. Available at:  
579 https://opendata.fmi.fi/wfs?request=GetCapabilities](https://opendata.fmi.fi/wfs?request=GetCapabilities)
- 580 Freeman, B. W. J., Evans, C. D., Musarika, S., Morrison, R., Newman, T. R., Page, S. E., Wiggs, G. F. S., Bell, N. G. A.,  
581 Styles, D., Wen, Y., Chadwick, D. R., and Jones, D. L.: Responsible agriculture must adapt to the wetland character of mid-  
582 latitude peatlands, *Glob. Change Biol.*, 28, 3795–3811, <https://doi.org/10.1111/gcb.16152>, 2022.
- 583 Gregersen, P. L., Culetic, A., Boschian, L., and Krupinska, K.: Plant senescence and crop productivity, *Plant Mol. Biol.*, 82,  
584 603–622, <https://doi.org/10.1007/s11103-013-0013-8>, 2013.
- 585 Guenther, A., Barthelmes, A., Huth, V., Joosten, H., Jurasinski, G., Koebisch, F., and Couwenberg, J.: Prompt rewetting of  
586 drained peatlands reduces climate warming despite methane emissions, *Nat. Commun.*, 11, 1644–1644,  
587 <https://doi.org/10.1038/s41467-020-15499-z>, 2020.
- 588 Harris, Z. M., Alberti, G., Viger, M., Jenkins, J. R., Rowe, R., McNamara, N. P., and Taylor, G.: Land-use change to  
589 bioenergy: grassland to short rotation coppice willow has an improved carbon balance, *GCB Bioenergy*, 9, 469–484,  
590 <https://doi.org/10.1111/gcbb.12347>, 2017.
- 591 Hiraishi, T., Krug, T., Tanabe, K., Srivastava, N., Baasansuren, J., Fukuda, M., and Troxler, T. G.: Supplement to the 2006  
592 IPCC guidelines for national greenhouse gas inventories: Wetlands, IPCC, Switzerland, 2014.
- 593 Honkanen, H., Kekkonen, H., Heikkinen, J., Kaseva, J., and Lång, K.: Minor effects of no-till treatment on GHG emissions  
594 of boreal cultivated peat soil, *Biogeochemistry*, <https://doi.org/10.1007/s10533-023-01097-w>, 2023.
- 595 Huang, Y., Ciais, P., Luo, Y., Zhu, D., Wang, Y., Qiu, C., Goll, D. S., Guenet, B., Makowski, D., De Graaf, I., Leifeld, J.,  
596 Kwon, M. J., Hu, J., and Qu, L.: Tradeoff of CO<sub>2</sub> and CH<sub>4</sub> emissions from global peatlands under water-table drawdown,  
597 *Nat. Clim. Change*, 11, 618–622, <https://doi.org/10.1038/s41558-021-01059-w>, 2021.
- 598 Humpenöder, F., Karstens, K., Lotze-Campen, H., Leifeld, J., Menichetti, L., Barthelmes, A., and Popp, A.: Peatland  
599 protection and restoration are key for climate change mitigation, *Environ. Res. Lett.*, 15, 104093,  
600 <https://doi.org/10.1088/1748-9326/abae2a>, 2020.
- 601 Jacquemart, A.-L.: *Vaccinium Uliginosum* L., *J. Ecol.*, 84, 771–785, <https://doi.org/10.2307/2261339>, 1996.
- 602 Jokinen, P., Pirinen, P., Kaukoranta, J.-P., Kangas, A., Alenius, P., Eriksson, P., Johansson, M., and Wilkman, S.: Tilastoja  
603 Suomen ilmastosta ja merestä 1991-2020, Ilmatieteen laitos, 2021.
- 604 Kandel, T. P., Elsgaard, L., and Laerke, P. E.: Measurement and modelling of CO<sub>2</sub> flux from a drained fen peatland  
605 cultivated with reed canary grass and spring barley, *Glob. Change Biol. Bioenergy*, 5, 548–561,  
606 <https://doi.org/10.1111/gcbb.12020>, 2013.
- 607 Kandel, T. P., Karki, S., Elsgaard, L., Labouriau, R., and Laerke, P. E.: Methane fluxes from a rewetted agricultural fen  
608 during two initial years of paludiculture, *Sci. Total Environ.*, 713, 136670–136670,  
609 <https://doi.org/10.1016/j.scitotenv.2020.136670>, 2020.
- 610 Karki, S., Elsgaard, L., Audet, J., and Laerke, P. E.: Mitigation of greenhouse gas emissions from reed canary grass in  
611 paludiculture: effect of groundwater level, *Plant Soil*, 383, 217–230, <https://doi.org/10.1007/s11104-014-2164-z>, 2014.
- 612 Kasimir, Å., He, H., Coria, J., and Nordén, A.: Land use of drained peatlands: Greenhouse gas fluxes, plant production, and  
613 economics, *Glob. Change Biol.*, 24, 3302–3316, <https://doi.org/10.1111/gcb.13931>, 2018.

- 614 Keck, H., Meurer, K. H. E., Jordan, S., Kätterer, T., Hadden, D., and Grelle, A.: Setting-aside cropland did not reduce  
615 greenhouse gas emissions from a drained peat soil in Sweden, *Front. Environ. Sci.*, 12,  
616 <https://doi.org/10.3389/fenvs.2024.1386134>, 2024.
- 617 Kutzbach, L., Schneider, J., Sachs, T., Giebels, M., Nykanen, H., Shurpali, N. J., Martikainen, P. J., Alm, J., and Wilmking,  
618 M.: CO<sub>2</sub> flux determination by closed-chamber methods can be seriously biased by inappropriate application of linear  
619 regression, *Biogeosciences*, 4, 1005–1025, <https://doi.org/10.5194/bg-4-1005-2007>, 2007.
- 620 Lammirato, C., Wallman, M., Weslien, P., Klemetsson, L., and Rütting, T.: Measuring frequency and accuracy of annual  
621 nitrous oxide emission estimates, *Agric. For. Meteorol.*, 310, 108624, <https://doi.org/10.1016/j.agrformet.2021.108624>,  
622 2021.
- 623 Lätti, A. K., Jaakola, L., Riihinen, K. R., and Kainulainen, P. S.: Anthocyanin and Flavonol Variation in Bog Bilberries  
624 (*Vaccinium uliginosum* L.) in Finland, *J. Agric. Food Chem.*, 58, 427–433, <https://doi.org/10.1021/jf903033m>, 2010.
- 625 Lehtonen, H., Huan-Niemi, E., and Niemi, J.: The transition of agriculture to low carbon pathways with regional  
626 distributive impacts, *Environ. Innov. Soc. Transit.*, 44, 1–13, <https://doi.org/10.1016/j.eist.2022.05.002>, 2022.
- 627 Leifeld, J. and Menichetti, L.: The underappreciated potential of peatlands in global climate change mitigation strategies,  
628 *Nat. Commun.*, 9, 1071–1071, <https://doi.org/10.1038/s41467-018-03406-6>, 2018.
- 629 Leppelt, T., Dechow, R., Gebbert, S., Freibauer, A., Lohila, A., Augustin, J., Droesler, M., Fiedler, S., Glatzel, S., Hoeper,  
630 H., Jaerveoja, J., Laerke, P. E., Maljanen, M., Mander, U., Maekiranta, P., Minkkinen, K., Ojanen, P., Regina, K., and  
631 Stromgren, M.: Nitrous oxide emission budgets and land-use-driven hotspots for organic soils in Europe, *Biogeosciences*,  
632 11, 6595–6612, <https://doi.org/10.5194/bg-11-6595-2014>, 2014.
- 633 Liu, W., Fritz, C., Van Belle, J., and Nonhebel, S.: Production in peatlands: Comparing ecosystem services of different land  
634 use options following conventional farming, *Sci. Total Environ.*, 875, 162534,  
635 <https://doi.org/10.1016/j.scitotenv.2023.162534>, 2023.
- 636 LLOYD, J. and TAYLOR, J.: On the Temperature-Dependence of Soil Respiration, *Funct. Ecol.*, 8, 315–323,  
637 <https://doi.org/10.2307/2389824>, 1994.
- 638 Lohila, A., Aurela, M., Regina, K., and Laurila, T.: Soil and total ecosystem respiration in agricultural fields: effect of soil  
639 and crop type, *Plant Soil*, 251, 303–317, <https://doi.org/10.1023/A:1023004205844>, 2003.
- 640 Lohila, A., Aurela, M., Tuovinen, J., and Laurila, T.: Annual CO<sub>2</sub> exchange of a peat field growing spring barley or  
641 perennial forage grass, *J. Geophys. Res.-Atmospheres*, 109, D18116–D18116, <https://doi.org/10.1029/2004JD004715>,  
642 2004.
- 643 Long, S. P. and Hällgren, J.-E.: Measurement of CO<sub>2</sub> assimilation by plants in the field and the laboratory, in:  
644 *Photosynthesis and Production in a Changing Environment: A field and laboratory manual*, edited by: Hall, D. O., Scurlock,  
645 J. M. O., Bolhàr-Nordenkamp, H. R., Leegood, R. C., and Long, S. P., Springer Netherlands, Dordrecht, 129–167,  
646 [https://doi.org/10.1007/978-94-011-1566-7\\_9](https://doi.org/10.1007/978-94-011-1566-7_9), 1993.
- 647 Maljanen, M., Liikanen, A., Silvola, J., and Martikainen, P.: Measuring N<sub>2</sub>O emissions from organic soils by closed  
648 chamber or soil/snow N<sub>2</sub>O gradient methods, *Eur. J. Soil Sci.*, 54, 625–631, <https://doi.org/10.1046/j.1365-2389.2003.00531.x>, 2003.
- 650 Maljanen, M., Hytonen, J., Makiranta, P., Alm, J., Minkkinen, K., Laine, J., and Martikainen, P. J.: Greenhouse gas  
651 emissions from cultivated and abandoned organic croplands in Finland, *Boreal Environ. Res.*, 12, 133–140, 2007.
- 652 Maljanen, M., Sigurdsson, B. D., Guomundsson, J., Oskarsson, H., Huttunen, J. T., and Martikainen, P. J.: Greenhouse gas  
653 balances of managed peatlands in the Nordic countries - present knowledge and gaps, *Biogeosciences*, 7, 2711–2738,  
654 <https://doi.org/10.5194/bg-7-2711-2010>, 2010.
- 655 Mander, U., Espenberg, M., Melling, L., and Kull, A.: Peatland restoration pathways to mitigate greenhouse gas emissions  
656 and retain peat carbon, *BIOGEOCHEMISTRY*, <https://doi.org/10.1007/s10533-023-01103-1>, 2023.
- 657 Meek, D. W., Hatfield, J. L., Howell, T. A., Idso, S. B., and Reginato, R. J.: A Generalized Relationship between  
658 Photosynthetically Active Radiation and Solar Radiation1, *Agron. J.*, 76, 939–945,  
659 <https://doi.org/10.2134/agronj1984.00021962007600060018x>, 1984.

- 660 Mitsch, W. J. and Wilson, R. F.: Improving the Success of Wetland Creation and Restoration with Know-How, Time, and  
661 Self-Design, *Ecol. Appl.*, 6, 77–83, <https://doi.org/10.2307/2269554>, 1996.
- 662 Morrison, R., Rowe, R. L., Cooper, H. M., and McNamara, N. P.: Multi-year carbon budget of a mature commercial short  
663 rotation coppice willow plantation, *GCB Bioenergy*, 11, 895–909, <https://doi.org/10.1111/gcbb.12608>, 2019.
- 664 Nielsen, C. K., Elsgaard, L., Jørgensen, U., and Lærke, P. E.: Soil greenhouse gas emissions from drained and rewetted  
665 agricultural bare peat mesocosms are linked to geochemistry, *Sci. Total Environ.*, 896, 165083,  
666 <https://doi.org/10.1016/j.scitotenv.2023.165083>, 2023.
- 667 Pacaldo, R. S., Volk, T. A., and Briggs, R. D.: Carbon Sequestration in Fine Roots and Foliage Biomass Offsets Soil CO<sub>2</sub>  
668 Effluxes along a 19-year Chronosequence of Shrub Willow (*Salix x dasyclados*) Biomass Crops, *BioEnergy Res.*, 7, 769–  
669 776, <https://doi.org/10.1007/s12155-014-9416-x>, 2014.
- 670 Pasquet, S., Pellerin, S., and Poulin, M.: Three decades of vegetation changes in peatlands isolated in an agricultural  
671 landscape, *Appl. Veg. Sci.*, 18, 220–229, <https://doi.org/10.1111/avsc.12142>, 2015.
- 672 Patrignani, A. and Ochsner, T. E.: Canopeo: A Powerful New Tool for Measuring Fractional Green Canopy Cover, *Agron.*  
673 *J.*, 107, 2312–2320, <https://doi.org/10.2134/agnonj15.0150>, 2015.
- 674 Raich, J. W., Rastetter, E. B., Melillo, J. M., Kicklighter, D. W., Steudler, P. A., Peterson, B. J., Grace, A. L., Moore III, B.,  
675 and Vorosmarty, C. J.: Potential Net Primary Productivity in South America: Application of a Global Model, *Ecol. Appl.*, 1,  
676 399–429, <https://doi.org/10.2307/1941899>, 1991.
- 677 Regina, K., Syvasalo, E., Hannukkala, A., and Esala, M.: Fluxes of N<sub>2</sub>O from farmed peat soils in Finland, *Eur. J. Soil Sci.*,  
678 55, 591–599, <https://doi.org/10.1111/j.1365-2389.2004.00622.x>, 2004.
- 679 [Shepherd, M.J., Lindsey, L.E. and Lindsey, A.J. Soybean Canopy Cover Measured with Canopeo Compared with Light](#)  
680 [Interception. \*Agricultural & Environmental Letters\* 3: 180031. doi:10.2134/aerl2018.06.0031, 2018.](#)
- 681 Strack, M., Davidson, S. J., Hirano, T., and Dunn, C.: The Potential of Peatlands as Nature-Based Climate Solutions, *Curr.*  
682 *Clim. Change Rep.*, 8, 71–82, <https://doi.org/10.1007/s40641-022-00183-9>, 2022.
- 683 Tanneberger, F., Birr, F., Couwenberg, J., Kaiser, M., Luthardt, V., Nерger, M., Pfister, S., Oppermann, R., Zeitz, J., Beyer,  
684 C., van der Linden, S., Wichtmann, W., and Närmann, F.: Saving soil carbon, greenhouse gas emissions, biodiversity and  
685 the economy: paludiculture as sustainable land use option in German fen peatlands, *Reg. Environ. Change*, 22, 69,  
686 <https://doi.org/10.1007/s10113-022-01900-8>, 2022.
- 687 Viherä-Aarnio, A., Jyske, T., and Beuker, E.: Pajut biokiertotaloudessa - Materiaaleja, arvoaineita, ympäristöhyötyjä :  
688 Synteesiraportti, Luonnonvarakeskus, 2022.
- 689 Vuorinen, J. and Mäkitie, O.: The method of soil testing in use in Finland, Maatalouskoelaitoksen maatumkimusosasto,  
690 Helsinki, 44 pp., 1955.
- 691 Wilson, D., Blain, D., Couwenberg, J., Evans, C., Murdiyarso, D., Page, S., Renou-Wilson, F., Rieley, J., Strack, M., and  
692 Tuittila, E.: Greenhouse gas emission factors associated with rewetting of organic soils, *Mires Peat*, 14, 1–28, 2016.
- 693 Zheng, D., Hunt, E., and Running, S.: A daily soil temperature model based on air temperature and precipitation for  
694 continental applications, *Clim. Res.*, 2, 183–191, <https://doi.org/10.3354/cr002183>, 1993.

695